Open

Cell Death and Differentiation (2013) 20, 709–720

www.nature.com/cdd

SCAR/WAVE-mediated processing of engulfed apoptotic corpses is essential for effective macrophage migration in *Drosophila*

IR Evans[1], PA Ghai[1], V Urbančič[2], K-L Tan[1] and W Wood*[,1]

In vitro **studies have shown that SCAR/WAVE activates the Arp2/3 complex to generate actin filaments, which in many cell types are organised into lamellipodia that are thought to have an important role in cell migration. Here we demonstrate that SCAR is utilised by *Drosophila* macrophages to drive their developmental and inflammatory migrations and that it is regulated via the Hem/Kette/Nap1-containing SCAR/WAVE complex. SCAR is also important in protecting against bacterial pathogens and in wound repair as *SCAR* mutant embryos succumb more readily to both sterile and infected wounds. However, in addition to driving the formation of lamellipodia in macrophages, SCAR is required cell autonomously for the correct processing of phagocytosed apoptotic corpses by these professional phagocytes. Removal of this phagocytic burden by preventing apoptosis rescues macrophage lamellipodia formation and partially restores motility. Our results show that efficient processing of phagosomes is critical for effective macrophage migration *in vivo*. These findings have important implications for the resolution of macrophages from chronic wounds and the behaviour of those associated with tumours, because phagocytosis of debris may serve to prolong the presence of these cells at these sites of pathology.**
Cell Death and Differentiation (2013) **20,** 709–720; doi:10.1038/cdd.2012.166; published online 18 January 2013

Numerous *in vitro* studies have shown SCAR/WAVE to have an important role in the generation of actin-based structures thought to be required for cell motility;[1] fewer studies have addressed its role *in vivo*, particularly dynamically and in the context of individually migrating cells. *Drosophila* embryonic macrophages (hemocytes) are highly migratory and represent a relevant cell type to probe the regulation of the actin cytoskeleton,[2] not least because of their evolutionary relationship to vertebrate macrophages, in terms of their specification,[3] conserved mechanisms utilised to detect and engulf apoptotic cells[4] and their potent inflammatory responses to wounds.[5]

Hemocyte dispersal is crucial to embryogenesis as these cells are largely responsible for secretion of matrix[6] and removal of apoptotic corpses,[7] much like their vertebrate counterparts.[8] With dispersal controlled by PDGF- and Vegf-related factors (Pvfs),[9] matrix[10] and contact inhibition[11] and their ability to respond to apoptotic corpses, wounds and pathogens, hemocytes represent a tractable genetic system to probe signal integration,[2,12] understanding which would be of enormous assistance in developing therapies against diseases involving immune cell dysfunction.

Despite recent studies showing roles for Fascin and Ena in regulating the hemocyte actin cytoskeleton,[13,14] it remains an open question as to how the structures these actin regulators act on are generated in these cells. Previous studies using *Drosophila* S2 cells indicated a requirement for SCAR in the formation of actin-rich lamellae downstream of Nck and Rac;[15–17] nonetheless a role within hemocytes has not yet been shown.

Drosophila SCAR/WAVE belongs to the WASp family of actin nucleation promoters. Diverse upstream signals activate WASp family members to activate Arp2/3-dependent actin polymerisation; SCAR/WAVE is regulated as part of a pentameric complex downstream of Rac, phosphatidyl inositide lipids and the adaptor Nck.[18] Several studies suggest phosphorylation of SCAR is important, with phosphorylation of the C-terminal tail recently shown to modulate its activity in *Dictyostelium*.[19] Analysis of *SCAR* mutants in *Drosophila* previously revealed it to have an essential role in processes including oogenesis, cell division, gastrulation, axonal guidance and muscle development.[20,21]

Here we investigate the role of SCAR in hemocyte migration within the *Drosophila* embryo. SCAR is required by hemocytes for the formation of lamellipodia and efficient migration, including to epithelial wounds. Surprisingly, *SCAR* mutant hemocytes become highly vacuolated because of numerous phagocytic corpses within their cell bodies, uncovering a novel role in apoptotic cell clearance. Most importantly, removing this defect by blocking apoptotic cell death helped restore hemocyte motility, revealing that apoptotic cells can modulate the dynamic behaviour of macrophages *in vivo*.

[1]Department of Biology and Biochemistry, University of Bath, Claverton Down, Bath, UK
*Corresponding author: W Wood, Department of Biology and Biochemistry, University of Bath, Claverton Down, Bath, BA2 7AY, UK. Tel: 01225-386261; Fax: 01225-386779; E-mail: w.wood@bath.ac.uk
[2]Current address: Department of Physiology, Development and Neuroscience, University of Cambridge, Downing Street, Cambridge CB2 3DY, UK
Keywords: apoptosis; macrophage; *Drosophila*; SCAR/WAVE; migration; hemocyte
Abbreviations: H_2O_2, hydrogen peroxide; Pvf, PDGF- and Vegf-related factor; Pvr, PDGF- and Vegf-related receptor; VNC, ventral nerve cord
Received 24.8.12; revised 9.11.12; accepted 26.11.12; Edited by H Steller; published online 18.1.13

Results

***SCAR* is required autonomously within hemocytes for their developmental dispersal.** The dispersal of hemocytes during embryogenesis is co-dependent on development of the ventral nerve cord (VNC)[22] and the dynamics of these cells is strongly influenced by their surrounding environment.[13] Previously, Zallen *et al.*[21] found that maternal and zygotic (M/Z) $SCAR^{\Delta 37}$ mutants exhibited early embryonic lethality because of defects during blastodermal stages, whereas even M/Z mutants of the weak $SCAR^{k13811}$ allele gave rise to a highly deformed VNC by stage 14/15. Therefore, to analyse the role of SCAR in hemocyte motility within a relatively unperturbed environment, hemocyte migration was probed in zygotic $SCAR^{\Delta 37}$ mutants. By stage 13 of embryonic development, hemocytes normally occupy the length of the VNC (Figure 1a),[23] however, in $SCAR^{\Delta 37}$ mutants they were absent from the ventral side of several neuromeres (segments of the VNC), indicating a failure in their dispersal (Figure 1b). Hemocytes move along the VNC from both anterior and posterior ends, the latter population having first penetrated the germ band before its retraction;[24] dynamic imaging revealed that hemocytes from these two populations make contact at the boundary between segments 6 and 7 (4/10 movies) or 7 and 8 (6/10 movies) during stage 13 in wild types (Figures 1f and g; Supplementary Movie 1). In contrast, both posterior and anterior hemocytes were retarded in $SCAR^{\Delta 37}$ embryos, suggesting a general defect in hemocyte progression along the VNC (Figures 1f–h; Supplementary Movie 1).

To test whether SCAR was required cell autonomously, dominant-negative GFP-SCAR (dn SCAR)[20] was specifically expressed within hemocytes. Dn SCAR expression phenocopied the defects in hemocyte dispersal observed in $SCAR^{\Delta 37}$ mutants (Figures 1c–f), including the delay in both anterior and posterior populations. The presence of two copies of the dn SCAR transgene further enhanced this phenotype (Figures 1e and f). In addition, hemocyte-specific expression of wild-type SCAR completely rescued developmental migration defects in a $SCAR^{\Delta 37}$ mutant background (SCAR rescue), further demonstrating an autonomous requirement for SCAR (Figures 1d–f).

Hemocyte migration along the VNC is controlled by separation of the VNC from the epithelium and PDGF- and Vegf-related receptor (Pvr) signalling in response to Pvf ligands expressed at the midline.[9,22,25,26] Heterozygous Pvr^{1} mutants displayed defects in VNC progression; this phenotype was significantly enhanced in $SCAR^{\Delta 37}/Pvr^{1}$ transheterozygotes, revealing a strong genetic interaction between *SCAR* and *Pvr* (Figure 1i), consistent with SCAR operating downstream of Pvr during this phase of migration.

***SCAR* is required for the inflammatory response and motility of hemocytes.** *Drosophila* hemocytes mount rapid inflammatory responses to laser-induced epithelial wounds, responding to hydrogen peroxide (H_2O_2).[5,27] To test whether SCAR is necessary for this process, we laser wounded the ventral epithelium of stage 15 embryos just laterally to the midline, and assessed hemocyte recruitment 1 h later, finding a substantial reduction in hemocytes recruited to wounds in $SCAR^{\Delta 37}$ mutants compared with wild types (Figures 2a–d), demonstrating that SCAR is an important regulator of this *in vivo* inflammatory migration. Dynamic imaging indicated that the few hemocytes that did migrate to wounds in $SCAR^{\Delta 37}$ mutants did so at a reduced rate, but displayed an identical directionality to wild types (Figure 2e). This suggests SCAR does not have an important role in guiding hemocytes or sensing wound-induced damage cues, but instead powers their migration in response to those signals. Decreased hemocyte recruitment was not a consequence of an overall reduction in hemocyte numbers since by stage 15 there was a comparable number of hemocytes on the ventral midline in $SCAR^{\Delta 37}$ and wild-type embryos (data not shown; also see Figure 7). We also found no significant difference in the numbers of hemocytes in the field of view in wild-type and *SCAR* mutants immediately post-wounding when normalised according to the area of the field of view. Importantly, a statistically significant decrease in the numbers of hemocytes at wounds was maintained when these values were normalised against both wound size and density of hemocytes present immediately after wounding (data not shown), comparable to the decrease presented in Figure 2d.

Hemocytes remain motile following their dispersal, exhibiting contact-dependent repulsion at stage 15.[11] Tracking $SCAR^{\Delta 37}$ mutant hemocyte movement at this stage revealed a dramatic reduction in motility compared with wild types (Figures 3a, b and f); once again hemocyte directionality was unaffected by loss of *SCAR* (data not shown). Expression of wild-type SCAR specifically in hemocytes in a $SCAR^{\Delta 37}$ mutant background (SCAR rescue) significantly rescued hemocyte speed, demonstrating a cell autonomous requirement of SCAR for effective migration. Thus, SCAR is important in driving hemocyte motility during three crucial behaviours: dispersal, patrolling and inflammation.

***SCAR* regulates hemocyte morphology *in vivo*.** SCAR is an important activator of the Arp2/3 complex that has a key role in the formation of lamellipodia *in vitro*, structures considered to drive cell motility in many cell types.[1] To examine the influence of SCAR on morphology we imaged GFP- and mCherry-moesin-labelled hemocytes live. Wild-type hemocytes typically extend large, dynamic, F-actin-rich lamellipodia at stage 15 of development (Figures 3a' and a''). These lamellipodia contain Ena at their tips and Fascin-enriched F-actin bundles/microspikes extending radially from the cell body towards the periphery;[13,14] some of these microspikes extend beyond the leading edge to form filopodia (Figure 3a''). $SCAR^{\Delta 37}$ hemocytes exhibited a dramatic loss of lamellipodia and were instead dominated by long, motile filopodia-like protrusions (Figures 3b' and b''; Supplementary Movie 2), giving rise to a stellate morphology strongly reminiscent of SCAR-depleted S2 cells in culture.[15–17]

The effects of $SCAR^{\Delta 37}$ on lamellipodia were cell autonomous as lamellipodial area could be restored to wild-type levels in SCAR rescue hemocytes (Figures 3c', c'' and g). In addition, lamellipodial area was reduced in hemocytes expressing dn SCAR (Figure 3d and g), with a more severe phenotype observed in those carrying two copies of this transgene (Figure 3e).

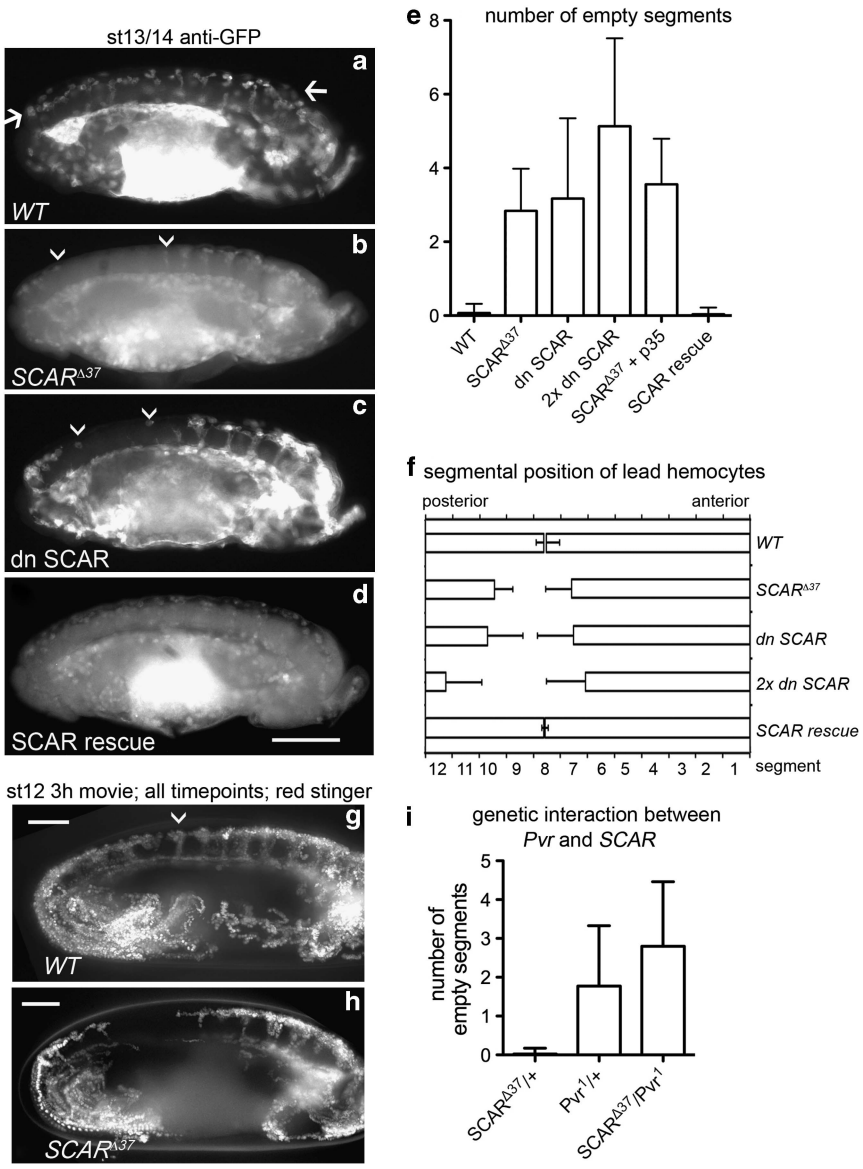

Figure 1 *SCAR* is required by migrating macrophages for their developmental dispersal and interacts genetically with *Pvr*. (**a–d**) Lateral views of stage 13/14 embryos immunostained to show distribution of GFP-labelled hemocytes. Hemocytes migrate from the head to form a single line atop the VNC in wild-type (WT) embryos (**a**); shown between arrows. Hemocytes failed to migrate as far in $SCAR^{\Delta 37}$ zygotic mutants (**b**) or when dominant-negative SCAR (dn SCAR) was specifically expressed in hemocytes (**c**). Regions between arrowheads indicate absence of hemocytes (**b** and **c**). Expression of wild-type SCAR specifically in hemocytes in a $SCAR^{\Delta 37}$ background (SCAR rescue) rescued this defect (**d**). (**e**) Quantification showing mean number of empty segments in fixed embryos at st13/14; each *SCAR* mutant, with the exception of SCAR rescue embryos, was significantly different from wild types ($P \leq 0.001$, Kruskal–Wallis test, Dunn's multiple comparison *post test*, $n \geq 29$ embryos per genotype), whereas hemocyte-specific expression of the anti-apoptotic gene p35 in a $SCAR^{\Delta 37}$ mutant background (SCAR + p35) failed to rescue. N.B. 2x dn SCAR represents a 50:50 mix of embryos with hemocytes expressing from 1 or 2 copies of UAS-dn SCAR (see Materials and methods section). (**f**) Quantification of mean position of lead hemocytes for anterior and posterior populations from fixed embryos; where hemocytes were present all along the VNC they were assumed to have met at segment 7.6, a value that corresponds to the mean meeting point taken from ten movies of WT embryos. (**g** and **h**) Projections of all time points of 3 h-long movies of WT and $SCAR^{\Delta 37}$ mutant embryos with red stinger-labelled hemocytes (see also Supplementary Movie 1) revealed that hemocytes from both posterior and anterior populations were retarded in $SCAR^{\Delta 37}$ mutants; hemocytes of these two populations met at the arrowhead in (**g**); representative of at least three movies per genotype. (**i**) Mean number of empty segments per embryo in $SCAR^{\Delta 37}/+$ and $Pvr^{1}/+$ heterozygotes and $SCAR^{\Delta 37}/Pvr^{1}$ transheterozygotes showing genetic interaction between Pvr^{1} and $SCAR^{\Delta 37}$. Each genotype is significantly different from the others ($P \leq 0.05$, Kruskal–Wallis test, Dunn's multiple comparison *post test*, $n \geq 35$ embryos per genotype). Anterior is to the right and ventral is up in all images; scale bars represent 50 μm; error bars represent the S.D.

Other members of the WASp family of nucleation promoting factors could be responsible for the formation of residual lamellipodia observed in $SCAR^{\Delta 37}$ mutants, particularly as WASp itself is recruited to *Dictyostelium* pseudopods in SCAR's absence.[28] However, neither *WASp* nor *WASH* appeared necessary for these residual lamellipodia because both $SCAR^{\Delta 37}$;$WASp^{EY06238}$ and $SCAR^{\Delta 37}$;$WASH^{\Delta 185}$ double mutants were indistinguishable from $SCAR^{\Delta 37}$ mutants in

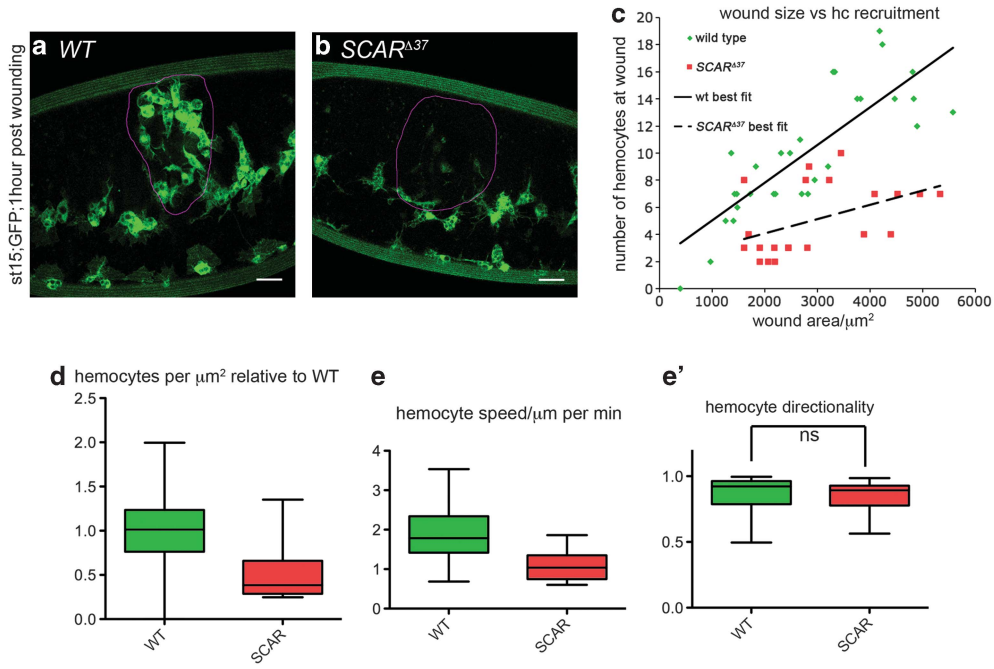

Figure 2 SCAR drives inflammatory migration of hemocytes. (**a** and **b**) Stage 15 wild-type (**a**) and *SCAR*$^{\Delta 37}$ mutant embryos (**b**) with GFP-labelled hemocytes (green) were wounded and imaged 1 h later (purple borders show wound position). (**c** and **d**) Scatter (**c**) and box and whisker plots (**d**) reveal that significantly fewer hemocytes were present per μm^2 of wound area in *SCAR*$^{\Delta 37}$ mutants ($P \leq 0.001$, *t*-test, $n \geq 20$ embryos per genotype). (**e**,**e'**) Box and whisker plots of hemocyte speed (**e**) and directionality (**e'**) show that *SCAR*$^{\Delta 37}$ mutant hemocytes migrated to wounds significantly more slowly ($P \leq 0.001$, *t*-test, 50 WT and 20 *SCAR*$^{\Delta 37}$ tracks taken from seven movies of each genotype), but as directionally as wild types (NS, not significant). Scale bars represent 20 μm. Lines represent the median, whereas boxes and whiskers show the interquartile and 2.5–97.5 percentile ranges, respectively, in these and all subsequent box and whisker plots

terms of lamellipodial area (Supplementary Figures 1 and 2). Any remaining lamellipodia may therefore be driven by maternal SCAR or a partially redundant mechanism.

Loss of SCAR function leads to defective phagosome processing. As hemocytes disperse through the embryo they engulf dying cells,[7] consequently containing numerous vacuoles by stage 15 (Figures 3a, h and 4a). Both *SCAR*$^{\Delta 37}$ mutant and dn SCAR hemocytes exhibited striking increases in the number of vacuoles per cell, especially when two copies of the dn SCAR transgene were present (compare Figure 3d and e), whereas SCAR rescue hemocytes were no more vacuolated than wild types (Figures 3c' and h). Acridine orange staining of wild-type and *SCAR*$^{\Delta 37}$ mutants showed the majority of these vacuoles contained apoptotic corpses (Figure 4b and f); this was validated by the absence of both vacuoles and acridine orange staining from apoptosis-null *H99* mutant embryos (Figure 4c and d), which lack the pro-apoptotic genes *hid*, *reaper* and *grim*.[29–31] This increase in engulfed apoptotic corpses was not due to increased levels of apoptosis because it was also observed in dn SCAR hemocytes and there was no increase in cell death in *SCAR*$^{\Delta 37}$ mutant embryos (Supplementary Figures 3a and b). Furthermore, hemocyte nuclei appeared morphologically similar to those in wild types and hemocyte-specific expression of the caspase inhibitor p35 (which can block autophagy and apoptosis)[32] failed to rescue vacuolation, lamellipodia and dispersal phenotypes in *SCAR*$^{\Delta 37}$ mutants (Figures 1e and 3h; Supplementary Figures 3c–g). In summary, increased vacuolation in *SCAR*$^{\Delta 37}$ mutants was not a consequence of hemocyte death or gross increases in apoptosis, thus uncovering a novel function for SCAR in the processing of phagocytosed apoptotic corpses.

To probe this role in phagocytic processing, a dominant-negative form of Rab5 was specifically expressed within hemocytes;[33] the Rab family of GTPases have important roles in trafficking, with Rab5 involved in phagosome maturation.[34] Dn Rab5-expressing hemocytes became highly vacuolated, phenocopying *SCAR*$^{\Delta 37}$ mutants (Figure 4g). Furthermore, the fraction of vacuoles within both dn Rab5 and *SCAR*$^{\Delta 37}$ mutant hemocytes that stained positively using LysoTracker, an indicator of phagosome acidification, was reduced compared with wild types (Figure 4h). In contrast, we found no striking accumulation of mCherry-Moesin around the persistent vacuoles observed in *SCAR* mutants suggesting that a failure to remove F-actin from the surfaces of vesicles, a process that precedes both Rab5 activation and subsequent acidification steps,[35] does not contribute to phagosomal maturation defects (Figure 4e; data not shown), whereas the dynamics of this process also appeared unaffected (data not shown). In summary, these results show SCAR as critical for the normal maturation and acidification of phagocytosed apoptotic corpses in macrophages *in vivo*.

Loss of the SCAR/WAVE complex component Hem phenocopies SCAR defects. The activity, stability and localisation of SCAR is regulated via incorporation into the evolutionarily conserved SCAR/WAVE complex, one component of which is Hem (also referred to as Kette or Nap1 in *Drosophila*).[16,17] *Drosophila Hem* mutants exhibit defects in

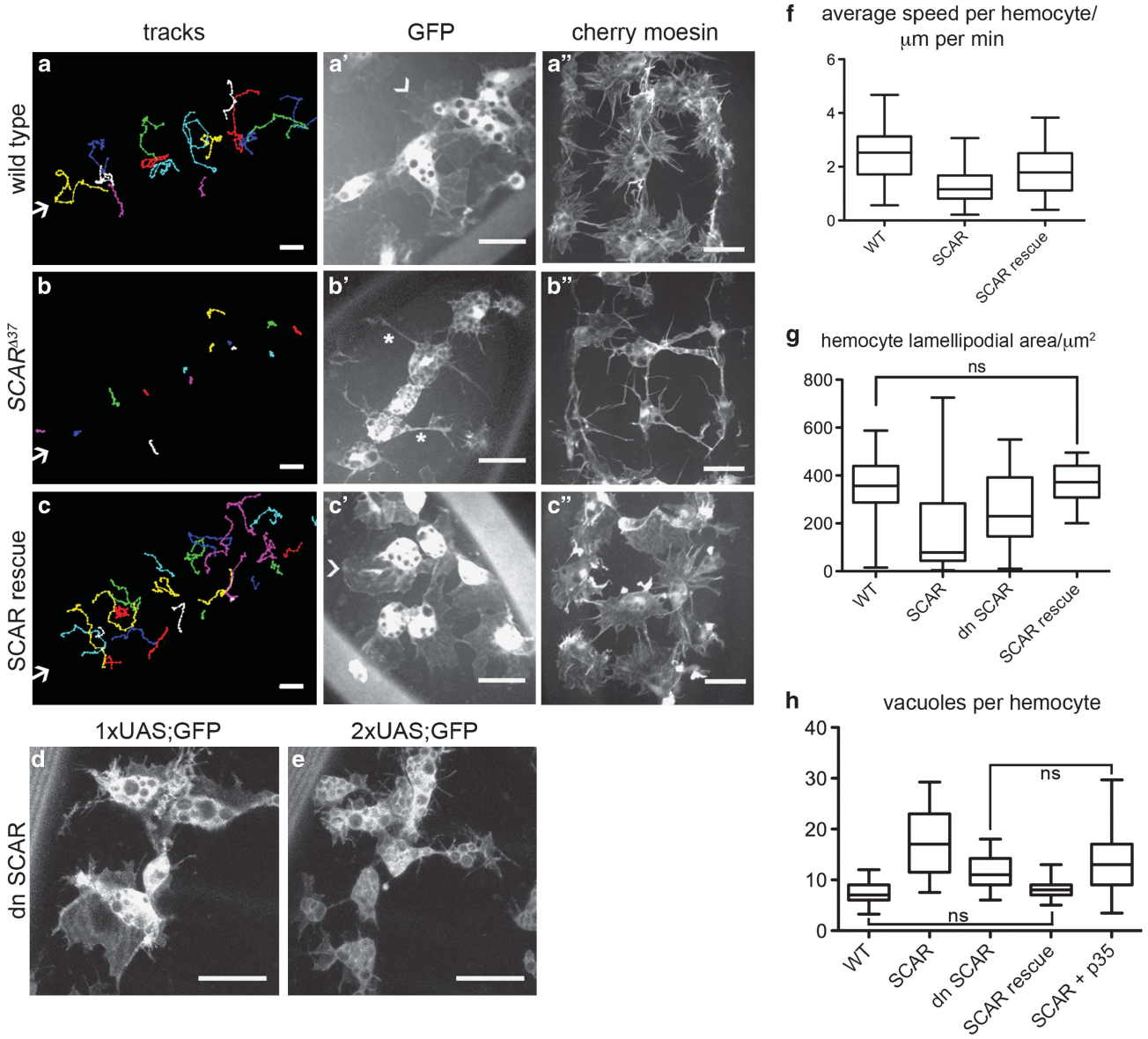

Figure 3 SCAR drives hemocyte migration and is necessary for normal hemocyte morphology. (**a**–**c**) Hemocyte tracks representing migration for 30 min at stage 15 in WT (**a**), *SCAR*$^{\Delta 37}$ (**b**) and SCAR rescue embryos (**c**); arrows show position of ventral midline. (**a'**–**c'**) Morphology of GFP-labelled hemocytes at stage 15 on the ventral midline; arrowheads illustrate large lamellipodia, asterisks indicate spindly protrusions. (**a''–c''**) F-actin morphology of hemocytes at the ventral midline shown via mCherry-moesin expression. (**d** and **e**) Hemocytes expressing GFP and dn SCAR from one UAS construct showed a mild reduction in lamellipodia (**d**), but a more severe phenotype was frequently seen in embryos that expressed dn SCAR from either 1 or 2 copies of the UAS insertion (**e**). (**f**–**h**) Box and whiskers plots showing quantification of hemocyte speeds (**f**; $n \geq 100$ hemocytes from ≥ 7 embryos per genotype) and lamellipodial area (**g**; $n \geq 25$ hemocytes from ≥ 15 embryos per genotype) and numbers of vacuoles per hemocyte (**h**; $n \geq 34$ hemocytes from ≥ 13 embryos per genotype); each category is significantly different from the rest ($P \leq 0.05$, one-way ANOVA, Bonferroni's *post test*), except where indicated (NS not significant). All scale bars represent 20 μm

axonal wiring and muscle cell fusion.[36,37] The same complex operates in vertebrates; in particular an almost exclusively haematopoietic-specific mouse homologue of Hem has a key role in neutrophil migration *in vitro*.[38] To verify the vacuolation phenotype and further understand the regulation of SCAR in hemocytes, we tested the role of Hem in hemocyte function. Analysis of *Hem*$^{J4\text{-}48}$ and *Hem*^{03335} mutants revealed *Hem* is necessary for normal dispersal (Figures 5a and b), migration at stage 15 (Figures 5c–e) and lamellipodia formation by hemocytes (Figures 5f–k). Similarly to *SCAR*$^{\Delta 37}$ mutants, *Hem* mutant hemocytes became highly vacuolated (Figures 5f–k). These data strongly suggest that SCAR is regulated via the SCAR/WAVE complex in hemocytes.

SCAR drives phagocytosis of bacteria and is necessary for efficient clearance of pathogens and damage repair to promote survival. One of the first functions ascribed to SCAR was in phagocytosis;[39] indeed SCAR is important in this regard in larval hemocytes.[40] To test whether SCAR

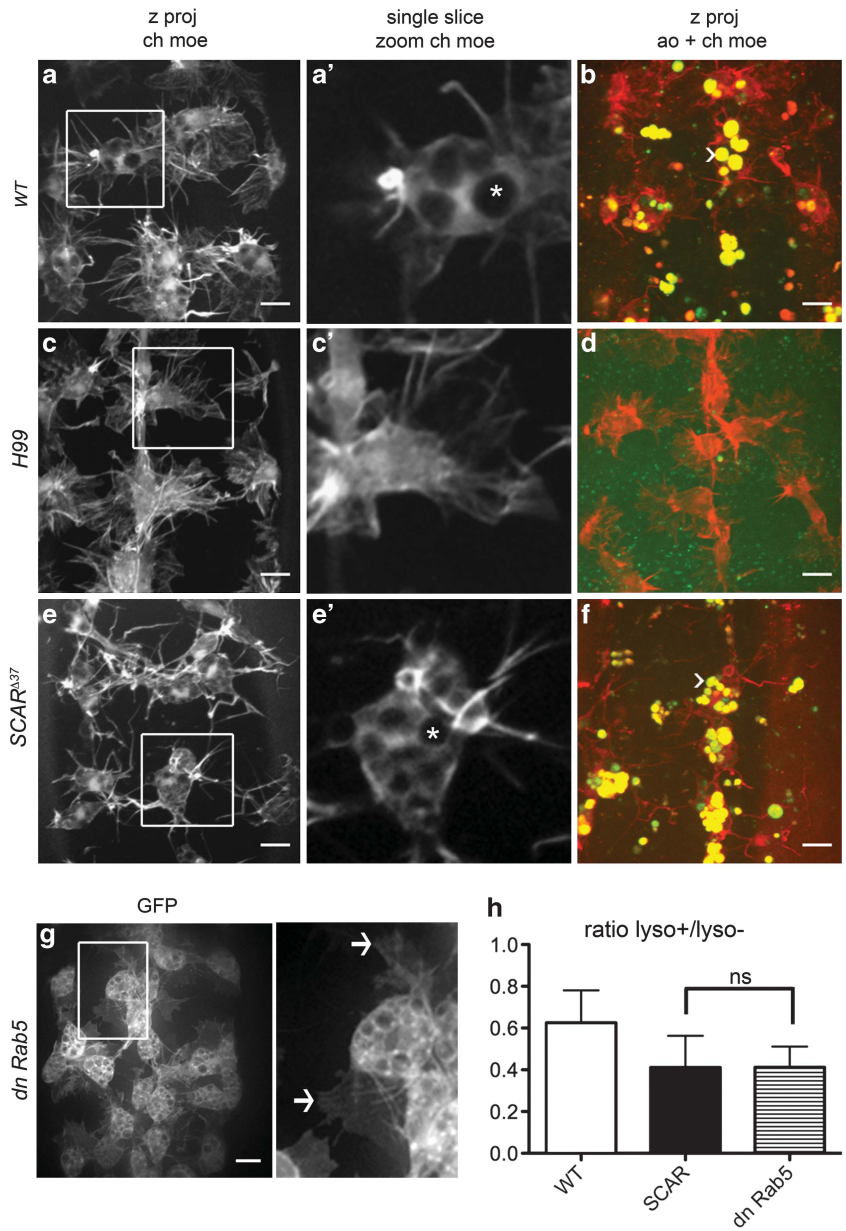

Figure 4 *SCAR* mutant hemocytes contain numerous apoptotic corpses and have defective phagosome processing. (**a** and **b**) Maximum projections (**a**) and zooms of single confocal slices from indicated box region (**a'**) reveal that vacuoles within mCherry-moesin-labelled (ch moe) wild-type (WT) hemocytes appear as regions excluding this F-actin marker (asterisks indicate examples); co-staining with acridine orange (ao = red and/or green spheres, arrowheads indicate examples; red = ch moe) shows that the majority of these vacuoles contain apoptotic corpses (**b**). (**c** and **d**) *H99* mutants neither contained vacuoles (**c**–**c'**), nor stained with acridine orange (**d**). (**e** and **f**) *SCAR*$^{\Delta 37}$ mutants were highly vacuolated (**e**–**e'**) and the majority of vacuoles stained positively for acridine orange (**f**). (**g**) Stage 15 hemocytes co-expressing dominant-negative Rab5 and GFP also became highly vacuolated, although they retained lamellipodia (indicated by arrows in zoomed region). (**h**) Quantification revealed that the mean fraction of vacuoles positively labelled with LysoTracker red within hemocytes per embryo was significantly reduced in both *SCAR*$^{\Delta 37}$ homozygotes and embryos that contained dn Rab-expressing hemocytes at stage 15 compared with wild types ($P \leq 0.01$, one-way ANOVA, Bonferroni's *post test*, $n \geq 12$ embryos per genotype); error bars represent the S.D.; scale bars show 10 μm. NS, not significant

carries out a similar function within embryos, RFP-expressing *E. coli* were microinjected into *SCAR*$^{\Delta 37}$ and wild-type stage 15 embryos containing GFP-labelled hemocytes. Live imaging 1 h post-injection revealed that *SCAR*$^{\Delta 37}$ mutant hemocytes phagocytosed *E. coli* at substantially reduced levels compared with wild types (Figures 6a–c). Non-phagocytosed bacteria were frequently observed adhered to the surface of *SCAR*$^{\Delta 37}$ mutant hemocytes, suggesting defects in phagocytosis rather than detection of bacteria.

The biological cost of defective clearance was probed by monitoring viability 24 h post-injection with the pathogenic bacteria *Erwinia carotovora carotovora 15* (*ecc15*). Infection with *ecc15* caused an increase in mortality in both wild types and *SCAR*$^{\Delta 37}$ mutants on top of that observed in PBS-injected

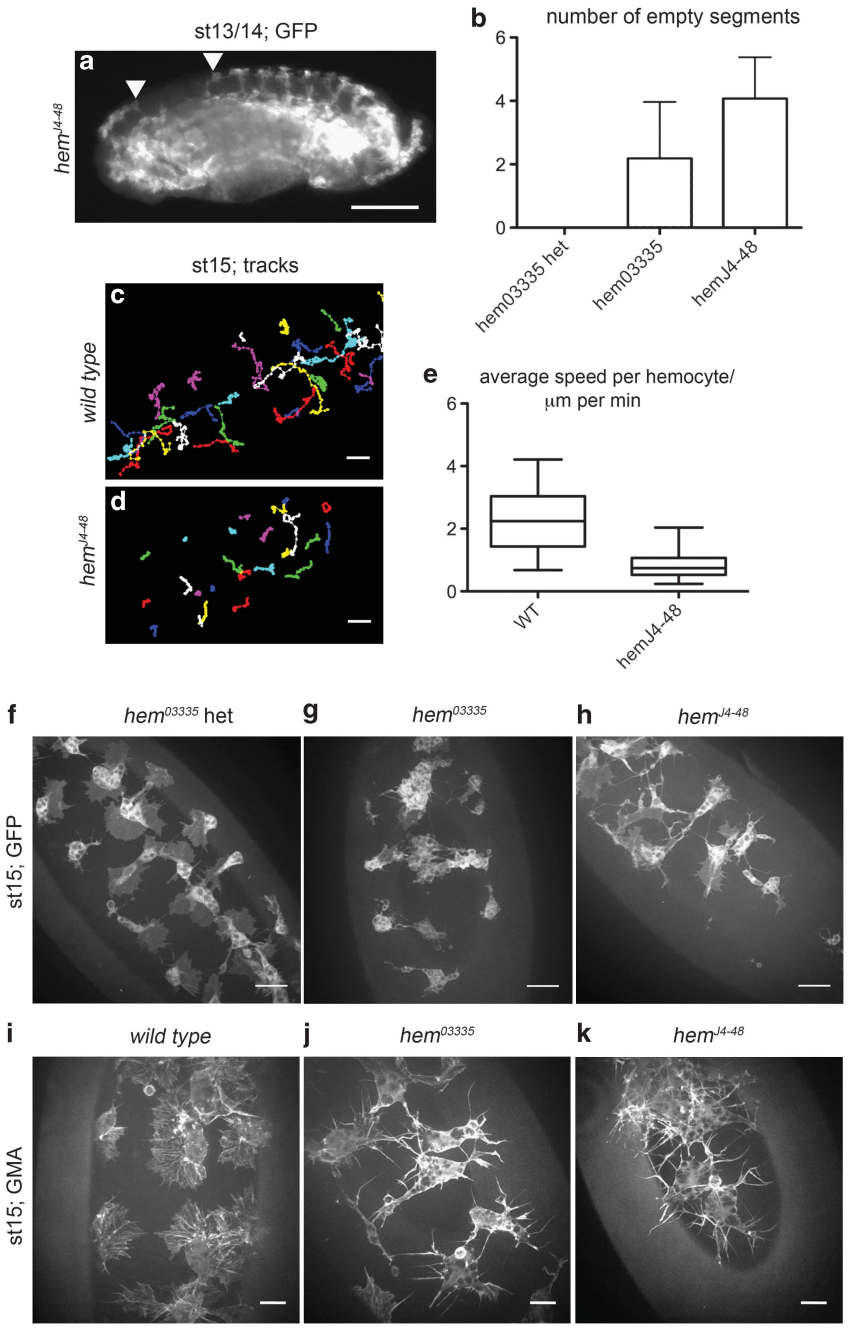

Figure 5 The SCAR complex component Hem is also required for lamellipodial formation and hemocyte migrations. (**a**) Immunostained stage 13/14 $Hem^{J4\text{-}48}$ mutant embryo with GFP-labelled hemocytes; hemocytes failed to occupy the entire length of the VNC (region bounded by arrowheads). (**b**) Quantification showing average number of segments devoid of hemocytes at stage 13/14 in Hem^{03335} heterozygotes and Hem^{03335} and $Hem^{J4\text{-}48}$ mutant embryos; error bars represent S.D.; each population is significantly different from the others ($P \leq 0.01$ Kruskal–Wallis test, Dunn's *post test*, $n \geq 30$ embryos per genotype). (**c** and **d**) Tracks of red stinger-labelled hemocytes migrating for 30 min over the VNC at stage 15 in wild-type (**c**) and $Hem^{J4\text{-}48}$ mutant embryos (**d**). (**e**) Box and whiskers plot showing average speed per hemocyte; speeds were significantly different ($P \leq 0.0001$, *t*-test, $n \geq 92$ hemocytes from six embryos per genotype). (**f–k**) GFP and GMA-labelled hemocytes at stage 15 at the ventral midline in indicated genotypes revealing that *Hem* is required for lamellipodia and its absence leads to vacuolation; anterior is up. Scale bars represent 50 μm (**a**), 20 μm (**c** and **d, f-h**) and 10 μm (**i–k**)

controls, but crucially this mortality was significantly enhanced in $SCAR^{\Delta 37}$ mutants (Figure 6d), indicating that failures in SCAR-dependent phagocytosis substantially compromised innate immune responses. Interestingly, there was a significant reduction in the viability of $SCAR^{\Delta 37}$ mutants when non-injected and PBS-injected embryos were compared (Figure 6d), paralleling the defects in larval healing observed on RNAi of SCAR,[41] and suggesting that SCAR has an important role in repair processes. To further confirm that *ecc15* and not simply the injection process itself accounted for

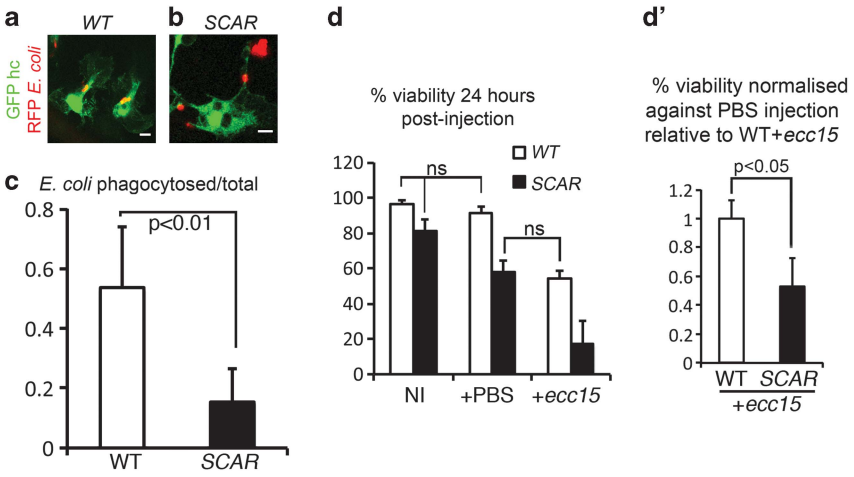

Figure 6 *SCAR* mutants exhibit defects in clearance of bacteria and damage repair and have enhanced susceptibility to pathogens. (**a** and **b**) Stage 15 embryos with GFP-labelled hemocytes (green) were injected with RFP-labelled *E. coli* (red) and imaged 1 h later (**a** and **b**), revealing a defect in phagocytosis in $SCAR^{\Delta 37}$ mutants (**b**) compared with wild types (**a**). (**c**) Bar graph showing mean ratio of phagocytosed *E. coli*:total *E. coli* in field of view at 1 h post-injection; there was a significant reduction in the amount of *E. coli* phagocytosed in $SCAR^{\Delta 37}$ mutants ($P<0.01$, Mann–Whitney test, $n\geq 4$ per genotype). (**d**) Bar graph showing mean viability of non-injected controls (NI) and embryos injected with PBS or *ecc15*; each column is significantly different ($P<0.01$, one-way ANOVA, Bonferroni's *post test*, $n=3$-4 with ≥ 100 embryos injected per experiment), except where indicated (NS), suggesting that $SCAR^{\Delta 37}$ mutants exhibit defects in repair of damage caused by injection and are more susceptible to *ecc15*-induced death. (**d'**) Normalising according to the percentage of embryos that hatch following injection with PBS and then expressing this value relative to the WT + *ecc15* condition shows that the enhanced lethality of *SCAR* mutants on injection with *ecc15* was not a consequence of their increased susceptibility to damage ($P<0.05$, Student's *t*-test). Scale and error bars represent 5 μm and the S.D., respectively. NS, not significant

the enhanced drop in survival, we normalised according to the appropriate PBS-injected control, which conclusively showed that, despite a decreased tolerance to the injection process, there was a further drop in survival because of the presence of *ecc15* (Figure 6d') and presumably its defective clearance.

Separating vacuolation and lamellipodial phenotypes in *SCAR* mutants. Loss of SCAR results in two clear defects: failure in the processing of apoptotic corpses and dramatic reductions in lamellipodial area. To investigate the contribution of the failure in phagosome processing to lamellipodial and motility defects in $SCAR^{\Delta 37}$ mutants we analysed $SCAR^{\Delta 37}$;*H99* double mutants, which lack all apoptosis. Strikingly, removal of the apoptotic clearance burden rescued both migration along the VNC and lamellipodial area to the levels observed in wild-type and *H99* mutant hemocytes (Figures 7a–f).

SCAR;*H99* double mutant hemocytes moved significantly faster than $SCAR^{\Delta 37}$ mutants at stage 15, but did not move as quickly as either SCAR rescue hemocytes (compare speeds with Figure 3g) or *H99* mutants (Figure 7g). Importantly, this partial rescue of hemocyte migration at stage 15 in $SCAR^{\Delta 37}$;*H99* double mutants revealed that, whereas vacuolation is a major contributing factor to the hemocyte motility defects observed in $SCAR^{\Delta 37}$ mutants, it cannot be the sole explanation.

In order to examine the nature of the rescued lamellipodia in more detail, the rate of lamellipodial area change was calculated from timelapse movies of wild-type hemocytes, the occasional $SCAR^{\Delta 37}$ mutant hemocytes that possessed large lamellipodia and $SCAR^{\Delta 37}$;*H99* double mutant hemocytes at stage 15. Of those hemocytes analysed, there was no difference in average lamellipodial areas (data not shown), however, $SCAR^{\Delta 37}$ mutant lamellipodia were more dynamic with greater changes in lamellipodial area over time, indicating a reduction in their stability. Surprisingly, the presence of the *H99* deficiency reverted lamellipodial behaviour in these *SCAR* mutant cells to that observed in wild types (Figure 7h). Therefore, even the occasional lamellipodia that appear morphologically normal in $SCAR^{\Delta 37}$ mutant hemocytes behave very differently to wild-type lamellipodia and this altered behaviour can be dramatically rescued simply by removing apoptosis, further highlighting the delicate balance between the machineries controlling phagosome processing and migration.

Discussion

SCAR has long been thought to drive the activation of the Arp2/3 complex to generate actin structures to drive migration. Here, we show that SCAR is crucial for the generation of lamellipodia in macrophages *in vivo*, structures whose presence is critical for effective motility of these cells to a variety of cues including H_2O_2 and Pvfs. SCAR is necessary for inflammatory responses and hemocyte dispersal, a process necessary for embryogenesis and immune surveillance. However, lamellipodial defects aside, the absence of SCAR causes an extreme vacuolation phenotype, which appears to be a consequence of a failure to adequately process ingested material, resulting in a build-up of undigested apoptotic corpses. Suppression of apoptosis and the consequent relief of this clearance burden prevents vacuolation and in turn completely rescues lamellipodia and partially restores normal migration speeds. How might increased vacuolation suppress cell motility in *SCAR* mutants? One potential explanation might involve sequestration/titration of

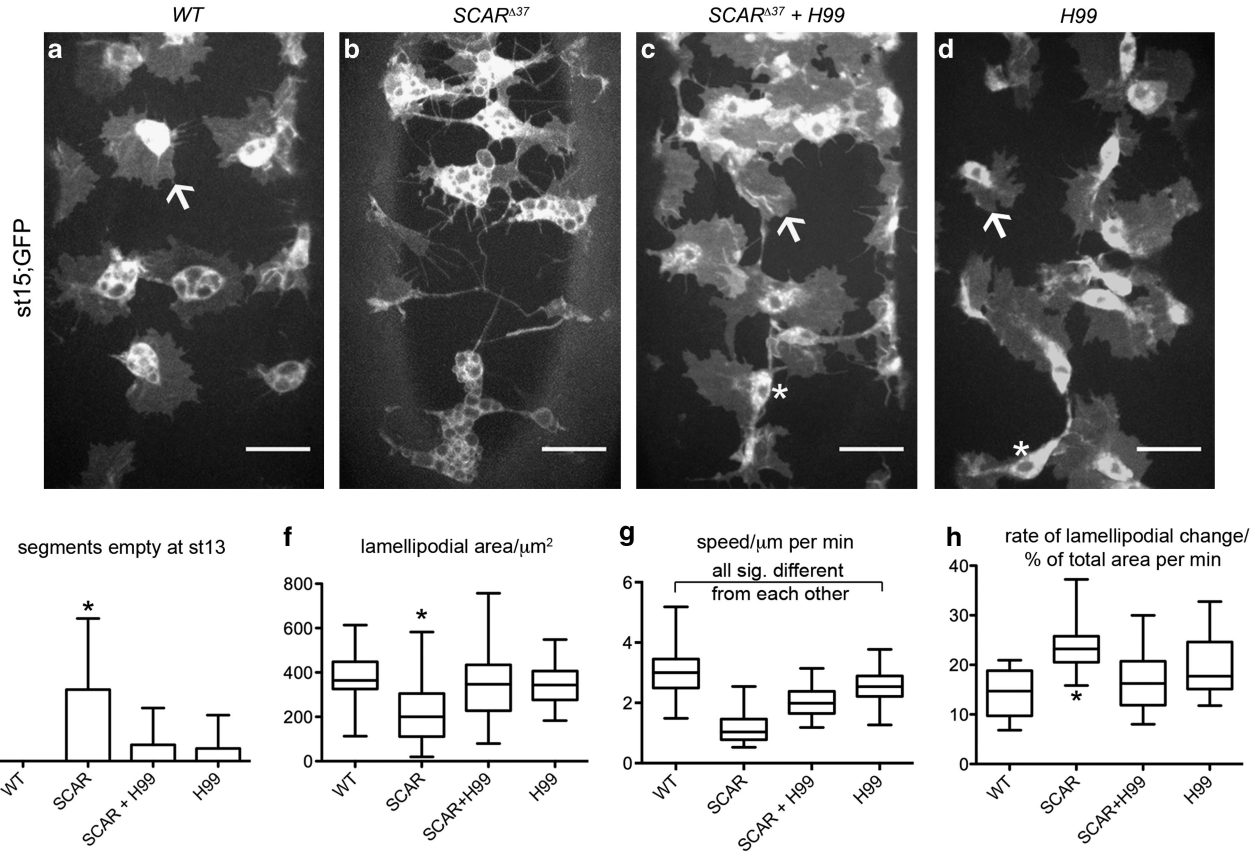

Figure 7 Removing apoptosis rescues lamellipodia and partially rescues speed in *SCAR* mutant hemocytes. (**a–d**) GFP expression in hemocytes at stage 15 in wild-type (**a**), $SCAR^{\Delta 37}$ (**b**), $SCAR^{\Delta 37}$;*H99* double mutant (**c**) and *H99* mutant (**d**) embryos revealed that the *H99* deficiency rescued lamellipodia (arrows). Regions with reduced levels of GFP in cell bodies in (**c**) and (**d**) are nuclei (asterisks); scale bars represent 20 μm. (**e**) Bar graph showing mean number of segments lacking hemocytes at stage 13; error bars represent the S.D. $SCAR^{\Delta 37}$ mutants exhibited a significant defect compared with the other genotypes ($P \leq 0.01$; Kruskal–Wallis test, Dunn's multiple comparison *post test*, $n \geq 15$ embryos per genotype), whereas there were no significant differences amongst the remaining comparisons. (**f–h**) Box and whisker plots of hemocyte lamellipodial area (**f**; $n > 50$ hemocytes from ≥ 12 embryos per genotype), speed (**g**; $n \geq 90$ hemocytes from ≥ 5 embryos per genotype) and rate of lamellipodial change per hemocyte per min (**h**; > 12 hemocytes were analysed from three different movies) at stage 15. Asterisks indicate a significant difference between $SCAR^{\Delta 37}$ mutants and the other genotypes in (**f**) ($P \leq 0.001$) and with WT and *SCAR;H99* in (**h**) ($P \leq 0.01$). *P*-values determined by one-way ANOVA and Bonferroni's *post test* (**f–h**)

components that would otherwise be able to rescue these defects. Proteomic characterisation of phagosomes has shown recruitment of SCAR and Ena[42] and the latter regulates lamellipodial dynamics and migration in hemocytes.[13] However, unlike the *H99* deficiency, overexpression of Ena in *SCAR* mutants failed to rescue migration along the VNC, whereas ena^{GC1} failed to interact genetically with *SCAR* in transheterozygous embryos (data not shown). It remains possible that rescue is via the presence of low levels of maternal SCAR that would otherwise be held at vacuoles.

An alternative hypothesis is that competition for the Arp2/3 complex by another activator on the surface of vacuoles might prevent lamellipodial formation via residual SCAR. WASH is another member of the WASp family and can activate Arp2/3 downstream of Rho1;[43] in *Dictyostelium* WASH has a role in the removal of V-ATPase to facilitate neutralisation of vacuoles before expulsion of indigestible waste[44] and therefore blocking phagosome maturation could drive WASH's accumulation on vacuoles. However, *SCAR;WASH* double mutants showed no rescue of lamellipodia appearing to rule this hypothesis out. We were also unable to find any obvious hemocyte dispersal or morphological defects in $WASH^{\Delta 185}$ mutants (Supplementary Figure 2). Similarly, *SCAR;WASp* double mutants neither rescued nor further perturbed lamellipodia in hemocytes.

Other potential explanations as to how vacuolation might suppress migration include a reduced availability of membrane to add to protrusions, cell signalling feedback mechanisms or even steric hindrance of migration through constricted spaces. Alternatively, increased ingested material to process (for instance cholesterol) or other changes in cellular lipid composition/distribution (e.g., phosphoinositides) could underlie migratory defects associated with vacuolation in *SCAR* mutants. Further investigation is required to determine the precise molecular mechanisms underpinning this intriguing balance of power. The fact that the removal of the apoptotic clearance burden only partially restores migration speeds in *SCAR* mutant hemocytes demonstrates that none of these explanations can fully explain the motility defects in *SCAR* mutants and that SCAR is indeed necessary in cells that utilise lamellipodia to move as quickly as possible.

The severely defective lamellipodia observed on loss of SCAR function suggests that Arp2/3's primary activator in hemocytes is SCAR. That some F-actin persists and migration remains possible in the absence of SCAR seemingly indicates that other actin nucleators operate within hemocytes, but that the network that other actin regulators influence is overwhelmingly Arp2/3 dependent. A loss of lamellipodia on depletion of Arp2/3 has recently been demonstrated *in vitro* in fibroblasts, correlating with a reduction in their migratory capabilities.[45,46] Interestingly, cells lacking Arp2/3 moved more slowly but still chemotaxed efficiently towards soluble PDGF,[45] paralleling the slower but highly directional routes *SCAR* mutant hemocytes take towards H_2O_2 at wounds. In addition, Arp2/3-depleted cells exhibited increased protrusion and retraction rates,[46] consistent with the increased lamellipodial dynamism of *SCAR* mutant hemocytes (Figure 7h).

The phagocytic processing defect in *SCAR* mutants has not been reported previously, although a potentially related role for both SCAR and WASp downstream of Cip4/Toca in actin comet-driven movement of vesicles from the plasma membrane has been shown in S2 cells.[47] Cells in other assays of SCAR/WAVE function are unlikely to have been exposed to as many apoptotic corpses as hemocytes are during development; alternatively upstream roles in phagocytosis may have hidden downstream functions of SCAR in processing.

Our results highlight a fine balance between processing of phagocytosed debris and formation of actin-rich protrusions necessary for driving migration within macrophages. It has been well documented that exposure to apoptotic corpses can switch phagocytes from pro-inflammatory to anti-inflammatory phenotypes[48,49] and we have previously shown that apoptotic cells can dictate the direction in which macrophages will migrate and represent their most highly prioritised cue in the *Drosophila* embryo.[27] Here, we demonstrate that even after engulfment apoptotic corpses can influence the migration machinery in an inflammatory cell, highjacking key components of that machinery if the clearance burden becomes too great and thereby disabling the macrophages' migration programme. In light of these findings, it is now critical to understand further the mechanisms underlying this crosstalk between debris clearance and migration if we are to design therapeutics to stimulate macrophage resolution away from areas such as chronic wounds or tumours where levels of debris and cell death may be very high.

Materials and Methods

Fly genetics. Twi-Gal4 and Gal4-independent fluorescent balancers[50,51] were used to maintain mutant lines and discriminate homozygous mutant embryos. Fly lines were previously generated in the lab or obtained from the Bloomington Stock Centre (University of Indiana, IN, USA); lines unavailable from Bloomington were kindly sent by the labs that originally made them (see references below). *Srp-Gal4* (ref. 25), *crq-Gal4* (ref. 26) and *pxn-Gal4* (ref. 5) were used to drive expression of UAS constructs specifically in hemocytes. *UAS-GFP-SCAR*[20] and *UAS-Rab5 dn*[33] were used as dominant-negative constructs; *UAS-p35* (ref. 52) and *UAS-SCAR*[21] were used as rescue constructs; insertions of *UAS-GFP*, *UAS-mCherry-Moesin*[53] and *UAS-red stinger*[11] were used to visualise hemocyte morphology and dynamics. Mutant alleles used were $SCAR^{\Delta 137}$ (ref. 21), $Hem^{J4\text{-}48}$ (ref. 36), Hem^{03335} (ref. 54) and *Df(3L)H99* (ref. 31), $WASp^{EY06238}$ (ref. 55) and $WASH^{\Delta 1185}$ (ref. 56); see Supplementary Table 1 for a full list of genotypes used. $SCAR^{\Delta 137}$ was recombined with *srp-Gal4* (Figures 1–6) or *srp-Gal4,UAS-GFP* and *srp-Gal4,UAS-red stinger* (Figure 7).

Quantification of developmental migration. Fixation and subsequent immunostaining of embryos was carried out as per Evans *et al.*[22], using rabbit anti-GFP (Abcam, Cambridge, UK) as a primary antibody. The presence or absence of GFP- or red stinger-labelled hemocytes on the ventral side of the VNC was scored by eye in either live or fixed and immunostained embryos using a Leica MZ16F fluorescent dissection microscope with a 5X/0.50 PL APO objective (Leica, Wetzlar, Germany). Low magnification images of representative embryos were taken on the same microscope.

Live imaging. Embryos were mounted on slides via Scotch double-sided sticky tape (3M, Maplewood, MN, USA) in voltalef oil as previously described;[22] halocarbon oil 700 (Sigma, St Louis, MO, USA) may be used as an alternative as voltalef oil is no longer commercially available. All live imaging was carried out at $22 \pm 1\ ^{\circ}C$.

Timelapse movies of red stinger-labelled hemocytes at stage 15 were taken of ventrally orientated embryos on a Leica DMIRB inverted microscope fitted with an HCX PL APO 40X objective, with a z-stack of three slices that captured red stinger-labelled hemocytes moving between the epidermis and VNC collected every 30 s for 30 min using ImagePro software (Media Cybernetics, Bethesda, MD, USA). Movies to determine when anterior and posterior hemocytes met were taken on the same set-up using a Leica HC PL APO 20X/0.70 multi-immersion objective lens (with oil); embryos were mounted laterally at mid-stage 12 and a z-stack of five slices was taken every 2 min to capture hemocyte progression along the VNC.

Laser ablation of epithelial cells was performed as previously[13] on a Zeiss LSM510 confocal microscope with a Zeiss FLUAR 40X/1.3 oil DIC objective (Zeiss, Oberkochen, Germany). The number of GFP-labelled hemocytes at or in contact with the wound margin was quantified 1 h post-ablation, with wound area measured from widefield images of transmitted laser light (channel D) in NIH ImageJ (http://rsbweb.nih.gov/ij/index.html). To determine speed and directionality of migration movies were taken immediately after wounding with a z-stack of five images collected every 2 min for 1 h. All tracking was performed on maximal projections of timelapse movies using ImageJ (manual tracking and chemotaxis tool plugins).

Stills of fluorescently labelled hemocytes on the ventral midline were taken of ventrally orientated, stage 15 embryos on either a Zeiss LSM510 confocal microscope with a Zeiss FLUAR 40X/1.3 oil immersion DIC objective or a Leica DMI 6000B UltraVIEW VoX spinning disk confocal imaging system with an HCX PL APO 40X/1.30 oil immersion objective; images were captured using Volocity (Perkin Elmer, Waltham, MA, USA). The latter set-up was also used to determine lamellipodial dynamics with GFP-labelled hemocytes between the epidermis and VNC imaged every 30 s for 10 min.

Acridine orange and LysoTracker staining. Dechorionated embryos were transferred to a glass vial containing 500 ml heptane (Sigma) plus 500 ml 5 μg/ml acridine orange (Sigma) or 50 nM LysoTracker red DND-99 (Molecular Probes, Life Technologies, Carlsbad, CA, USA) in PBS (Sigma) and agitated for 5 or 30 min, respectively. Embryos were then removed from the interface in a minimal volume of fluid to halocarbon oil 700 and subsequently transferred in a small oil droplet to slides for immediate imaging. We found that acridine orange and LysoTracker both produced highly variable intensity of staining between embryos, even within the same treatment. It was therefore necessary to use different exposure times during image capture to avoid under/overexposure. Images were collected on the spinning disk system outlined above. To quantify acidification of phagosomes, the fraction of vacuoles $> 1.5\ \mu m$ in diameter within hemocytes with clear LysoTracker labelling was determined from single confocal slices (LysoTracker positive vacuoles/total vacuoles in field of view).

Image quantification and statistical analysis. Lamellipodial area (total area − cell body area) was measured manually in ImageJ from contrast-enhanced maximum projections of confocal stacks of hemocytes expressing cytoplasmic GFP; vitelline membrane autofluoresence was manually removed from more superficial (ventral) confocal slices where it obscured hemocyte morphology before assembly of projections. Only hemocytes lying in the pseudo-2D plane between epidermis and VNC, bounded by the edges of the VNC, which could be distinguished from their neighbours were analysed. The values herein are likely an under representation of *SCAR* phenotypes as the most severely affected hemocytes tended to clump together and thus eluded analysis. Vacuole numbers per hemocyte were determined by scanning though z-stacks of confocal images.

Lamellipodial dynamics were calculated as follows: the lamellipodial area of individual GFP-labelled hemocytes was determined every 30 s over the course of a

10 min movie (as described above). The absolute change in area (i.e., the modulus) between subsequent timepoints was then averaged per hemocyte and this was normalised according to the average lamellipodial area for that hemocyte over the entire movie to take into account differences in hemocyte size. For this analysis only *SCAR*$^{\Delta 37}$ mutant hemocytes with large lamellipodia were quantified.

Statistical analysis was performed using Graph Pad Prism for Mac (Graph Pad Software, La Jolla, CA, USA). In the box and whiskers plots, the lines represent the medians, whereas the boxes and whiskers show the interquartile and 2.5–97.5 percentile ranges, respectively.

Bacterial injections. *DH5α E. coli* and *ecc15* bacteria were grown for 18 h to stationary phase at 37 and 30 °C, respectively. After washing in sterile endotoxin-free PBS (Sigma), cultures were adjusted to the appropriate density (OD = 10 for *E. coli* and OD = 0.1 for *ecc15*) and microinjected into stage 15 embryos as per Vlisidou *et al.*,[57] injection of sterile, endotoxin-free PBS was used as a negative control. For analysis of phagocytosis, a coverslip was mounted over injected embryos and z-stacks with a 1 μm spacing of GFP-labelled hemocytes and RFP-labelled *E. coli* taken at 1 h post-injection using a Zeiss LSM510 confocal microscope and a PL APO 63X/1.4 oil immersion objective. These z-stacks were then used to calculate the percentage of phagocytosed *E. coli* per embryo. For viability studies, injected embryos were transferred to apple juice agar plates and stored at 25 °C in humid conditions. Viability was scored at 24 h post-injection based on larval hatching or movement.

Conflict of Interest

The authors declare no conflict of interest.

Acknowledgements. We thank Eyal Schejter (Weizman Institute of Science, Israel), Sergio Simoes and Jennifer Zallen (Memorial Sloan-Kettering Cancer Centre, USA), and Sven Bogdan (University of Munster, Germany) for fly lines; Isabella Vlisidou (University of Bath, UK) and Bruno Lemaitre (EPFL, Switzerland) kindly provided bacterial strains for this study. Guy Wiedermann (University of Dundee, UK) and James Lightfoot (University of Bristol, UK) performed preliminary characterisation of *SCAR* phenotypes as project students in the lab. This work would not be possible without the use of the Bioimaging facility maintained by Adrian Rogers (CEOS, University of Bath, UK), the Bloomington Stock Centre (University of Indiana, USA) and Flybase. We thank Brian Stramer (Kings College London, UK), Paul Whitley and Andrew Chalmers (University of Bath, UK) for helpful comments and advice. WW's lab is funded by the Wellcome Trust.

1. Insall RH, Machesky LM. Actin dynamics at the leading edge: from simple machinery to complex networks. *Dev Cell* 2009; **17**: 310–322.
2. Evans IR, Wood W. Understanding in vivo blood cell migration–Drosophila hemocytes lead the way. *Fly* 2011; **5**: 110–114.
3. Evans CJ, Hartenstein V, Banerjee U. Thicker than blood: conserved mechanisms in Drosophila and vertebrate hematopoiesis. *Dev Cell* 2003; **5**: 673–690.
4. Franc NC. Phagocytosis of apoptotic cells in mammals, Caenorhabditis elegans and Drosophila melanogaster: molecular mechanisms and physiological consequences. *Front Biosci-Landmrk* 2002; **7**: D1298–D1313.
5. Stramer B, Wood W, Galko MJ, Redd MJ, Jacinto A, Parkhurst SM *et al.* Live imaging of wound inflammation in Drosophila embryos reveals key roles for small GTPases during in vivo cell migration. *J Cell Biol* 2005; **168**: 567–573.
6. Olofsson B, Page DT. Condensation of the central nervous system in embryonic Drosophila is inhibited by blocking hemocyte migration or neural activity. *Dev Biol* 2005; **279**: 233–243.
7. Sears HC, Kennedy CJ, Garrity PA. Macrophage-mediated corpse engulfment is required for normal Drosophila CNS morphogenesis. *Development* 2003; **130**: 3557–3565.
8. Hopkinson-Woolley J, Hughes D, Gordon S, Martin P. Macrophage recruitment during limb development and wound healing in the embryonic and foetal mouse. *J Cell Sci* 1994; **107**(Pt 5): 1159–1167.
9. Cho NK, Keyes L, Johnson E, Heller J, Ryner L, Karim F *et al.* Developmental control of blood cell migration by the Drosophila VEGF pathway. *Cell* 2002; **108**: 865–876.
10. Urbano JM, Torgler CN, Molnar C, Tepass U, Lopez-Varea A, Brown NH *et al.* Drosophila laminins act as key regulators of basement membrane assembly and morphogenesis. *Development* 2009; **136**: 4165–4176.
11. Stramer B, Moreira S, Millard T, Evans I, Huang CY, Sabet O *et al.* Clasp-mediated microtubule bundling regulates persistent motility and contact repulsion in Drosophila macrophages in vivo. *J Cell Biol* 2010; **189**: 681–689.
12. Wood W, Jacinto A. Drosophila melanogaster embryonic haemocytes: masters of multitasking. *Nature reviews. Mol Cell Biol* 2007; **8**: 542–551.
13. Tucker PK, Evans IR, Wood W. Ena drives invasive macrophage migration in Drosophila embryos. *Disease Models Mechanisms* 2011; **4**: 126–134.
14. Zanet J, Stramer B, Millard T, Martin P, Payre F, Plaza S. Fascin is required for blood cell migration during Drosophila embryogenesis. *Development* 2009; **136**: 2557–2565.
15. Biyasheva A, Svitkina T, Kunda P, Baum B, Borisy G. Cascade pathway of filopodia formation downstream of SCAR. *J Cell Sci* 2004; **117**(Pt 6): 837–848.
16. Kunda P, Craig G, Dominguez V, Baum B. Abi, Sra1, and Kette control the stability and localization of SCAR/WAVE to regulate the formation of actin-based protrusions. *Curr Biol* 2003; **13**: 1867–1875.
17. Rogers SL, Wiedemann U, Stuurman N, Vale RD. Molecular requirements for actin-based lamella formation in Drosophila S2 cells. *J Cell Biol* 2003; **162**: 1079–1088.
18. Campellone KG, Welch MD. A nucleator arms race: cellular control of actin assembly. *Nature reviews. Mol Cell Biol* 2010; **11**: 237–251.
19. Ura S, Pollitt AY, Veltman DM, Morrice NA, Machesky LM, Insall RH. Pseudopod growth and evolution during cell movement is controlled through SCAR/WAVE dephosphorylation. *Curr Biol* 2012; **22**: 553–561.
20. Gildor B, Massarwa R, Shilo BZ, Schejter ED. The SCAR and WASp nucleation-promoting factors act sequentially to mediate Drosophila myoblast fusion. *EMBO Rep* 2009; **10**: 1043–1050.
21. Zallen JA, Cohen Y, Hudson AM, Cooley L, Wieschaus E, Schejter ED. SCAR is a primary regulator of Arp2/3-dependent morphological events in Drosophila. *J Cell Biol* 2002; **156**: 689–701.
22. Evans IR, Hu N, Skaer H, Wood W. Interdependence of macrophage migration and ventral nerve cord development in Drosophila embryos. *Development* 2010; **137**: 1625–1633.
23. Tepass U, Fessler LI, Aziz A, Hartenstein V. Embryonic origin of hemocytes and their relationship to cell death in Drosophila. *Development* 1994; **120**: 1829–1837.
24. Siekhaus D, Haesemeyer M, Moffitt O, Lehmann R. RhoL controls invasion and Rap1 localization during immune cell transmigration in Drosophila. *Nat Cell Biol* 2010; **12**: 605–610.
25. Bruckner K, Kockel L, Duchek P, Luque CM, Rorth P, Perrimon N. The PDGF/VEGF receptor controls blood cell survival in Drosophila. *Dev Cell* 2004; **7**: 73–84.
26. Wood W, Faria C, Jacinto A. Distinct mechanisms regulate hemocyte chemotaxis during development and wound healing in Drosophila melanogaster. *J Cell Biol* 2006; **173**: 405–416.
27. Moreira S, Stramer B, Evans I, Wood W, Martin P. Prioritization of competing damage and developmental signals by migrating macrophages in the Drosophila embryo. *Curr Biol* 2010; **20**: 464–470.
28. Veltman DM, King JS, Machesky LM, Insall RH. SCAR knockouts in Dictyostelium: WASP assumes SCAR's position and upstream regulators in pseudopods. *J Cell Biol* 2012; **198**: 501–508.
29. Chen P, Nordstrom W, Gish B, Abrams JM. grim, a novel cell death gene in Drosophila. *Genes Dev* 1996; **10**: 1773–1782.
30. Grether ME, Abrams JM, Agapite J, White K, Steller H. The head involution defective gene of Drosophila melanogaster functions in programmed cell death. *Genes Dev* 1995; **9**: 1694–1708.
31. White K, Grether ME, Abrams JM, Young L, Farrell K, Steller H. Genetic control of programmed cell death in Drosophila. *Science* 1994; **264**: 677–683.
32. Lee CY, Baehrecke EH. Steroid regulation of autophagic programmed cell death during development. *Development* 2001; **128**: 1443–1455.
33. Zhang J, Schulze KL, Hiesinger PR, Suyama K, Wang S, Fish M *et al.* Thirty-one flavors of Drosophila rab proteins. *Genetics* 2007; **176**: 1307–1322.
34. Kinchen JM, Ravichandran KS. Phagosome maturation: going through the acid test. *Nature reviews. Mol Cell Biol* 2008; **9**: 781–795.
35. Kitano M, Nakaya M, Nakamura T, Nagata S, Matsuda M. Imaging of Rab5 activity identifies essential regulators for phagosome maturation. *Nature* 2008; **453**: 241–245.
36. Hummel T, Leifker K, Klambt C. The Drosophila HEM-2/NAP1 homolog KETTE controls axonal pathfinding and cytoskeletal organization. *Genes Dev* 2000; **14**: 863–873.
37. Schroter RH, Lier S, Holz A, Bogdan S, Klambt C, Beck L *et al.* kette and blown fuse interact genetically during the second fusion step of myogenesis in Drosophila. *Development* 2004; **131**: 4501–4509.
38. Weiner OD, Rentel MC, Ott A, Brown GE, Jedrychowski M, Yaffe MB *et al.* Hem-1 complexes are essential for Rac activation, actin polymerization, and myosin regulation during neutrophil chemotaxis. *PLoS Biol* 2006; **4**: e38.
39. Seastone DJ, Harris E, Temesvari LA, Bear JE, Saxe CL, Cardelli J. The WASp-like protein scar regulates macropinocytosis, phagocytosis and endosomal membrane flow in Dictyostelium. *J Cell Sci* 2001; **114**(Pt 14): 2673–2683.
40. Pearson AM, Baksa K, Ramet M, Protas M, McKee M, Brown D *et al.* Identification of cytoskeletal regulatory proteins required for efficient phagocytosis in Drosophila. *Microbes Infection/Institut Pasteur* 2003; **5**: 815–824.
41. Lesch C, Jo J, Wu Y, Fish GS, Galko MJ. A targeted UAS-RNAi screen in Drosophila larvae identifies wound closure genes regulating distinct cellular processes. *Genetics* 2010; **186**: 943–957.
42. Stuart LM, Boulais J, Charriere GM, Hennessy EJ, Brunet S, Jutras I *et al.* A systems biology analysis of the Drosophila phagosome. *Nature* 2007; **445**: 95–101.

43. Liu R, Abreu-Blanco MT, Barry KC, Linardopoulou EV, Osborn GE, Parkhurst SM. Wash functions downstream of Rho and links linear and branched actin nucleation factors. *Development* 2009; **136**: 2849–2860.
44. Carnell M, Zech T, Calaminus SD, Ura S, Hagedorn M, Johnston SA *et al.* Actin polymerization driven by WASH causes V-ATPase retrieval and vesicle neutralization before exocytosis. *J Cell Biol* 2011; **193**: 831–839.
45. Wu C, Asokan SB, Berginski ME, Haynes EM, Sharpless NE, Griffith JD *et al.* Arp2/3 is critical for lamellipodia and response to extracellular matrix cues but is dispensable for chemotaxis. *Cell* 2012; **148**: 973–987.
46. Suraneni P, Rubinstein B, Unruh JR, Durnin M, Hanein D, Li R. The Arp2/3 complex is required for lamellipodia extension and directional fibroblast cell migration. *J Cell Biol* 2012; **197**: 239–251.
47. Fricke R, Gohl C, Dharmalingam E, Grevelhorster A, Zahedi B, Harden N *et al.* Drosophila Cip4/Toca-1 integrates membrane trafficking and actin dynamics through WASP and SCAR/WAVE. *Curr Biol* 2009; **19**: 1429–1437.
48. Fadok VA, Bratton DL, Konowal A, Freed PW, Westcott JY, Henson PM. Macrophages that have ingested apoptotic cells in vitro inhibit proinflammatory cytokine production through autocrine/paracrine mechanisms involving TGF-beta, PGE2, and PAF. *J Clin Invest* 1998; **101**: 890–898.
49. Voll RE, Herrmann M, Roth EA, Stach C, Kalden JR, Girkontaite I. Immunosuppressive effects of apoptotic cells. *Nature* 1997; **390**: 350–351.
50. Halfon MS, Gisselbrecht S, Lu J, Estrada B, Keshishian H, Michelson AM. New fluorescent protein reporters for use with the Drosophila Gal4 expression system and for vital detection of balancer chromosomes. *Genesis* 2002; **34**: 135–138.
51. Le T, Liang Z, Patel H, Yu MH, Sivasubramaniam G, Slovitt M *et al.* A new family of Drosophila balancer chromosomes with a w- dfd-GMR yellow fluorescent protein marker. *Genetics* 2006; **174**: 2255–2257.
52. Hay BA, Wolff T, Rubin GM. Expression of baculovirus P35 prevents cell death in Drosophila. *Development* 1994; **120**: 2121–2129.
53. Millard TH, Martin P. Dynamic analysis of filopodial interactions during the zippering phase of Drosophila dorsal closure. *Development* 2008; **135**: 621–626.
54. Baumgartner S, Martin D, Chiquet-Ehrismann R, Sutton J, Desai A, Huang I *et al.* The HEM proteins: a novel family of tissue-specific transmembrane proteins expressed from invertebrates through mammals with an essential function in oogenesis. *J Mol Biol* 1995; **251**: 41–49.
55. Li W, Baker NE. Engulfment is required for cell competition. *Cell* 2007; **129**: 1215–1225.
56. Linardopoulou EV, Parghi SS, Friedman C, Osborn GE, Parkhurst SM, Trask BJ. Human subtelomeric WASH genes encode a new subclass of the WASP family. *Plos Genet* 2007; **3**: e237.
57. Vlisidou I, Dowling AJ, Evans IR, Waterfield N, ffrench-Constant RH, Wood W. Drosophila embryos as model systems for monitoring bacterial infection in real time. *Plos Pathog* 2009; **5**: e1000518.

Supplementary Information accompanies this paper on Cell Death and Differentiation website (http://www.nature.com/cdd)